Optical bistability and hysteresis of hybrid metal-semiconductor nano-dimer

A. V. Malyshev[1, 2, 3, *] and V. A. Malyshev[3, 4]

[1] *GISC, Departamento de Física de Materiales, Universidad Complutense, E-28040 Madrid, Spain*
[2] *Ioffe Physical-Technical Institute, 26 Politechnicheskaya str., 194021 St.-Petersburg, Russia*
[3] *Centre for Theoretical Physics and Zernike Institute for Advanced Materials, University of Groningen, Nijenborgh 4, 9747 AG Groningen, The Netherlands*
[4] *St. Petersburg State University, 198504 St. Petersburg, Russia*

(Dated: June 9, 2011)

Optical response of an artificial composite nano-dimer comprising a semiconductor quantum dot and a metal nanosphere is analyzed theoretically. We show that internal degrees of freedom of the system can manifest bistability and optical hysteresis as functions of the incident field intensity. We argue that these effects can be observed for the real world systems, such as a CdSe quantum dot and an Au nanoparticle hybrids. These properties can be revealed by measuring the optical hysteresis of the Rayleigh scattering. We show also that the total dipole moment of the system can be switched abruptly between its two stable states by small changes in the excitation intensity. The latter promises various applications in the field of all-optical processing at nanoscale, the most underlying of them being the volatile optical memory.

PACS numbers: 78.67.-n

I. INTRODUCTION

Arrays of metallic nanoparticles (often referred to as plasmonic arrays), are widely recognized as potential building blocks for nanoscale optical circuitry[1–9] (see also Ref. 10 for an overview). Recently, a number of groups reported fascinating properties of artificial molecules comprised of a semiconductor quantum dot (SQD) in the proximity of a metallic nanoparticles (MNP).[11–19] Nonlinear Fano resonances[12,13] and bistability in the absorption spectrum,[13,14] control of the exciton emission of the SQD (inhibition or enhancement)[15] and variable quenching of the SQD photoluminescence by proximate gold nanoparticles,[11] as well as "meta-molecular" resonances,[16] the inhibition of optical excitation and enhancement of Rabi flopping,[17] tunable nanoswitching,[18] and gain without inversion[19] have been predicted. The role of the multipole SQD-MNP interaction in explaining the spectra of hybrid systems has been discussed in details in Ref. 20. All these effects depend on both geometrical parameters and material properties of hybrid clusters providing an excellent opportunity of more fine-grained control of spectral and dynamical properties of nanoscale objects.

We consider the simplest hybrid nano-cluster comprising a SQD and a spherical MNP – artificial hybrid diatomic nano-molecule. When such a system is excited optically, the dipole moment of the optical transition in the SQD generates an additional electric field at the MNP, which is superposed with the external field. Similarly, the induced dipole moment of the MNP generates an additional electric field in the SQD. Thus, the presence of the MNP leads to a self action (feedback) of the SQD. Together with nonlinearity of the SQD itself, this can give rise to a variety of new optical properties. In particular, if the coupling between two nanoparticles is strong enough, the self-action can result in optical bistability of the response. Note that a dimer comprised of strongly coupled two-level molecules can not manifest bistability.[21] Thus, a SQD-MNP hetero-dimer is a fascinating nanoscopic system exhibiting this feature.

To demonstrate the feasibility of the bistable optical response of hybrid composites, we consider a closely spaced CdSe (or CdSe/ZnSe) SQD and an Au nanosphere. We show that for a range of geometrical parameters of the system (SQD and MNP radii and center-to-center distance), the optical bistability and hysteresis can be observed in it. We argue also that because of the axial symmetry of such artificial diatomic molecule, its state can be switched not only by traditional change of the driving field amplitude, but also by changing the incoming field polarization with respect to the molecule axis, which offers an additional mechanism of control. The fact that both the SQD and the MNP can sustain high electric fields suggests such possible applications of artificial molecules as all-optical switches and optical memory cells at nanoscale in the visible; the two stable states of the systems have different total dipole moments, providing a possibility to store information in this degree of freedom.

The paper is organized as follows. In the next Section the model and formalism are described. In Sec. III we present the standard steady-state analysis of the bistable optical response, which gives rise to the optical hysteresis addresses in the Section IV. We discuss possible applications of the predicted effects in Sec. V while Section VI summarizes the paper.

II. FORMALISM

We assume that the SQD-MNP hybrid molecule is embedded in a dielectric host with the permittivity ε_b and is driven by a linearly polarized external electric field with

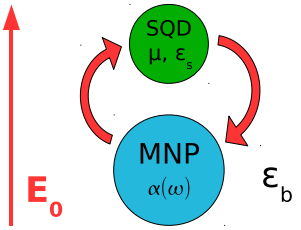

FIG. 1: Schematics of the hybrid SQD-MNP system embedded into a homogeneous dielectric background with the permittivity ε_b and subjected to an external field with an amplitude $\mathbf{E}_0$. The SQD optical transition dipole moment and the semiconductor dielectric constant are denoted as $\boldsymbol{\mu}$ and ε_s, respectively, while $\alpha(\omega)$ is the MNP polarizability. The curved arrows symbolize the dipole-dipole SQD-MNP interaction.

an amplitude $\mathbf{E}_0$ and frequency ω. Figure 1 shows the schematics of the system. The SQD is modeled as a two level system with the transition frequency ω_0 and optical transition dipole moment $\boldsymbol{\mu}$. It is treated quantum mechanically within the framework of the Maxwell-Bloch equations for the 2×2 density matrix ρ_{mn} $(m,n=0,1)$. The MNP is considered classically; the response of the MNP is described by its frequency dependent scalar polarizability within the point dipole approximation (this can easily be generalized for the case of more complex shapes of the MNP by considering an appropriate polarizability tensor). All sizes of the system (the SQD and MNP radii and the SQD-MNP center-to-center distance) are assumed to be small enough to neglect the retardation effects and to consider both particles as point dipoles. The rotating wave approximation is used throughout the paper, so that all time dependent quantities represent amplitudes of the corresponding characteristics of SQD, the set of equations for which reads:

$$\dot{Z} = -\gamma\,(Z+1) - \frac{1}{2}\left[\,\Omega\,R^* + \Omega^* R\,\right]\ , \tag{1a}$$

$$\dot{R} = -(i\,\Delta + \Gamma)\,R + \Omega\,Z\ , \tag{1b}$$

where $Z=\rho_{11}-\rho_{00}$ is the population difference between the SQD excited and ground states, R is the amplitude of the off-diagonal density matrix element defined through $\rho_{10} = -(i/2)R\exp(-i\omega t)$, γ and Γ are the relaxation constant of the population and the dipole dephasing, respectively, $\Delta=\omega_0-\omega$ is the detuning of the driving field from the SQD resonance, and $\Omega=\boldsymbol{\mu}\mathbf{E}/\hbar$ is the electric field (in frequency units) acting *inside* the SQD. The field acting upon the SQD is equal to the sum of the external field $\mathbf{E}_0$ and the field produced by the induced dipole moment $\mathbf{P}_{\rm MNP}$ of the MNP. The field $\mathbf{E}$ *inside* the SQD is reduced by the factor $\varepsilon_s' = (\varepsilon_s+2\varepsilon_b)/(3\varepsilon_b)$ where ε_s is the permeability of the SQD (see e. g. Ref. 22 or Ref. 23, Ch. V, p. 138):

$$\mathbf{E} = \frac{1}{\varepsilon_{\rm s}'}\left(\mathbf{E}_0 + \frac{\widehat{\mathbf{S}}\,\mathbf{P}_{\rm MNP}}{\varepsilon_b\,d^3}\right)\ . \tag{2}$$

Here, $\widehat{\mathbf{S}} = {\rm diag}(-1,-1,2)$ is the angular part of the dipole field Green's tensor (z axis being parallel to the system axis), d is the SQD-MNP center-to-center distance while $\mathbf{P}_{\rm MNP}$ is given by:

$$\mathbf{P}_{\rm MNP} = \varepsilon_b\,\alpha(\omega)\left(\mathbf{E}_0 + \frac{\widehat{\mathbf{S}}\,\mathbf{P}_{\rm SQD}}{\varepsilon_b\,d^3}\right)\ , \tag{3}$$

where $\alpha(\omega) = a^3\,\gamma(\omega)$ is the classical frequency dependent polarizability of the MNP, a being its radius, $\gamma(\omega) = [\varepsilon_M(\omega)-\varepsilon_b]/[\varepsilon_M(\omega)+2\varepsilon_b]$, and $\varepsilon_M(\omega)$ is the dielectric function of the metal. We do not take into account the corrections to the polarizability due to the depolarization shift and radiative damping,[24] which are negligible for nanoparticle sizes of our interest ($\leq$10 nm). The second term in the parenthesis of Eq. (3) is the field produced by the SQD dipole moment $\mathbf{P}_{\rm SQD} = -i\boldsymbol{\mu}\,R$ at the MNP.

The exciton radius in CdSe is about 5 nm[25] while the typical radius of the considered SQD is about $1.5-2$ nm, so the wavefunctions involved in the optical transition are extended over the whole dot. In deriving Eq. (3) we used therefore the approximation of the homogeneous electric polarization of the whole SQD volume. In this case the dipole field around the SQD is screened by the bare background dielectric constant only.[22] Note that the dipole moment $\mathbf{P}_{\rm SQD}$ is calculated quantum mechanically and accounts for the screening which results from the SQD dielectric response (see below). Finally, for the total electric field *inside* the SQD we obtain:

$$\mathbf{E} = \frac{1}{\varepsilon_{\rm s}'}\left[\mathbf{1} + \frac{\gamma(\omega)\,a^3}{d^3}\,\widehat{\mathbf{S}}\right]\mathbf{E}_0 + \frac{\gamma(\omega)\,a^3}{\varepsilon_b\,\varepsilon_s'\,d^6}\,\widehat{\mathbf{S}}^2\,\mathbf{P}_{\rm SQD}\ . \tag{4}$$

As is seen from Eq. (4), the presence of the MNP results in two effects: the first term accounts for the renormalization of the external field amplitude $\mathbf{E}_0$ while the second represents the self-action of the SQD via the MNP; the field inside the SQD depends on the dipole moment of the SQD itself.

The effect of the self-action on the dynamics of the SQD-MNP hybrid nano-molecule can be revealed after substituting Eq. (4) into Eq. (1b) and representing Ω in the form

$$\Omega = \widetilde{\Omega}_0 - i\,G\,R \tag{5}$$

with $\widetilde{\Omega}_0$ and G given by

$$\widetilde{\Omega}_0 = \frac{1}{\varepsilon_s'}\left[1 + \frac{a^3\gamma(\omega)}{d^3}\,\frac{\boldsymbol{\mu}\,\widehat{\mathbf{S}}\,\mathbf{E}_0}{\hbar\Omega_0}\right]\Omega_0\ , \tag{6a}$$

$$G = \frac{\gamma(\omega)\,a^3}{\varepsilon_b\,\varepsilon_s'\,\hbar\,d^6}\,\boldsymbol{\mu}\,\widehat{\mathbf{S}}^2\,\boldsymbol{\mu}\ , \tag{6b}$$

where $\Omega_0 = \boldsymbol{\mu}\mathbf{E}_0/\hbar$ is the Rabi frequency of the bare external field, $\widetilde{\Omega}_0$ is the renormalized Rabi frequency and G

is the feedback parameter. The latter absorbs all information governing the SQD self-action, such as, material constants, geometry of the system or details of the interaction (*e. g.* contributions of higher multipoles[20]).

In a number of recent publications dealing with the same system, a different formula for the constant G was used in which the factor $\varepsilon'_{\rm s}$ appears squared in the denominator of the G.[12–20] The second factor $\varepsilon'_{\rm s}$ is supposed to take into account the screening of the dipole field by the SQD dielectric response. We note, however, that it is the product $G\,R$ that determines the latter field and, as can be seen from Eq. (8b), $R \propto \widetilde{\Omega}_0 \propto \Omega_0/\varepsilon'_{\rm s}$, so the dipole field $G\,R$ is already additionally screened.

The feedback G is the most important parameter of the theory; once it is calculated it determines the nonlinear properties of the SQD response. Using Eq. (5), Eq. (1b) can be rewritten in the following form:

$$\dot{R} = -[(\Gamma - G_{\rm I}\,Z) + i\,(\Delta + G_{\rm R}\,Z)]\,R + \widetilde{\Omega}_0\,Z \qquad (7)$$

with $G_{\rm R} = {\rm Re}(G)$ and $G_{\rm I} = {\rm Im}(G)$. From Eq. (7) two consequences of the SQD self-action become apparent: (i) - the renormalization of the SQD resonance frequency $\omega_0 \mapsto \omega_0 + G_{\rm R}\,Z$ and (ii) - the renormalization of the dipole dephasing rate $\Gamma \mapsto \Gamma - G_{\rm I}\,Z$. Both renormalized quantities depend on the population difference Z. Similar renormalizations originate from the local field correction in the nonlinear optical response of dense gaseous assemblies of two-level systems,[26] optically dense thin films,[27] and linear molecular aggregates.[28] The population dependencies of the SQD resonance frequency and the dipole dephasing rate provide a feedback mechanism, which results in a number of fascinating effects.

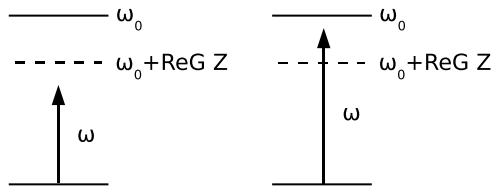

FIG. 2: Two possible types of the SQD excitation. Left plot – the excitation frequency ω lies below the renormalized SQD transition frequency $\omega_0 - G_{\rm R}$ ($\Delta > G_{\rm R}$); as Z increases with the excitation the system is driven further out of resonance. Right plot: $\omega > \omega_0 - G_{\rm R}$ ($\Delta < G_{\rm R}$); the excitation drives the system into the resonance which favors the bistability to occur.

Let us assume that both $G_{\rm R} > 0$ and $G_{\rm I} > 0$, which is the case for a CdSe SQD conjugated with a golden MNP. Then the renormalized resonance frequency *increases* with the excitation intensity, ranging from $\omega_0 - G_{\rm R}$ ($Z = -1$ in the ground state) to $\omega_0 + G_{\rm R}$ ($Z = 1$ in the excited state). In this case the response of the system depends on the relative position of the excitation frequency ω with respect to the renormalized SQD transition frequency $\omega_0 - G_{\rm R}$. Thus, if $\omega < \omega_0 - G_{\rm R}$ or equivalently $\Delta > G_{\rm R}$ (see Fig. 2, left plot) then the excitation is driving the SQD out of resonance, so that the SQD is becoming less absorptive. Contrary to that, if $\omega > \omega_0 - G_{\rm R}$ or $\Delta < G_{\rm R}$ (see Fig. 2, right plot) the SQD is being driven into the self-sustaining resonance by the incoming field. That is the case of the positive loopback. In this case, apart from the usual linear "weak field" solution, the second kind of a stable state can turn up, which results from the above-mentioned positive feedback mechanism. We show below that the latter has a threshold character, giving rise to bistability and hysteresis of the system response characteristics.

III. STEADY-STATE ANALYSIS

First, we analyze Eq. (1a) and Eq. (1b) under steady-state conditions ($\dot{Z} = \dot{R} = 0$) to obtain stationary states of the system. The corresponding solutions read:

$$\frac{|\widetilde{\Omega}_0|^2}{\gamma\,\Gamma} = -\frac{Z+1}{Z}\,\frac{|(\Gamma - G_{\rm I}Z) + i\,(\Delta + G_{\rm R}Z)|^2}{\Gamma^2} \qquad (8a)$$

$$R = \frac{Z\,\widetilde{\Omega}_0}{(\Gamma - G_{\rm I}\,Z) + i\,(\Delta + G_{\rm R}\,Z)}\ . \qquad (8b)$$

Equation (8a) is of the third order in Z and therefore may have three real solutions, depending on values of Δ, Γ, $G_{\rm R}$, and $G_{\rm I}$. The same applies to the SQD dipole moment amplitude R.

Hereafter, we consider a CdSe SQD in the vicinity of an Au MNP and use the following set of parameters: the transition energy $\hbar\omega_0 = 2.36$ eV (which corresponds to the optical transition in a 3.3 nm SQD), the SQD dielectric constant $\varepsilon_s = 6.2$, the SQD transition dipole moment $\mu = 0.65$ e·nm,[12] the MNP radius $a = 10$ nm, the SQD-MNP center-to-center distance $d = 17$ nm, the host dielectric constant $\varepsilon_b = 1$, and the relaxation constants γ and Γ defined through $1/\gamma = 0.8$ ns and $1/\Gamma = 0.3$ ns.[13] To calculate the polarizability $\gamma(\omega)$ of the MNP, we used the tabulated data for the permittivity of gold from Ref. 29. For these parameters $G = G_{\rm R} + i\,G_{\rm I} = (25.4 + 10.6\,i)\,\Gamma$. Note that the frequency domain of our interest is a narrow region in the vicinity of the SQD resonance, with the width of about several units of Γ (see below), which is much smaller that the width of the MNP plasmonic resonance. We therefore neglected the frequency dependence of the MNP polarizability when calculating the feedback parameter G and used $\gamma(\omega) \approx \gamma(\omega_0)$.

Figure 3 shows the solution of Eq. (8a) and Eq. (8b) for the set of parameters specified above and different detunings Δ. As is seen from the plots, within a window of $-3.3\,\Gamma \le \Delta \le 13.8\,\Gamma$, the field dependence of Z and R, have three allowed values for a given intensity $|\Omega_0|^2/(\gamma\Gamma)$. The upper limit of the window, $\Delta = 13.8\,\Gamma$, corresponds to the excitation frequency $\omega = \omega_0 - 13.8\,\Gamma$

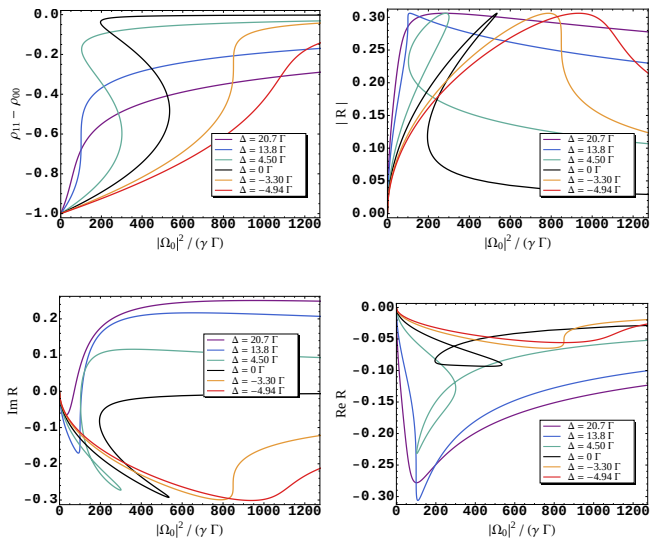

FIG. 3: Stationary solutions to Eq. (8a) and Eq. (8b) for a hybrid nano-molecule comprising a 3.3 nm CdSe SQD and 20 nm Au sphere separated by the center-to-center distance of 17 nm (other parameters are described in the text). The solutions are calculated for different detuning Δ as functions of the normalized external field intensity $\Omega_0/\sqrt{\gamma\Gamma}$. The upper row shows the population difference $Z = \rho_{11} - \rho_{00}$ (left) and the SQD dipole moment amplitude $|R|$ (right). The lower left panel displays the absorptive part of the dipole amplitude, $\mathrm{Im}(R)$, while the right one — its dispersive part, $\mathrm{Re}(R)$.

which lies above the renormalized SQD resonance frequency $\omega_0 - G_\mathrm{R} = \omega_0 - 25.4\,\Gamma$ (the positive loopback case). The lower limit of the window, $\Delta = -3.3\,\Gamma$, is negative and the corresponding frequency lies above the bare resonance. Nevertheless, the SQD can still be driven into the self-sustaining resonance by the external field. At larger ω (larger negative Δ), the resonance between the excitation and the SQD can not be attained because it requires a significant positive population difference Z that is unreachable under stationary conditions: due to the saturation effect, the upper limit for the population difference is $Z = 0$ in the steady state. Because of that, the bistability effect disappears for large negative detunings.

Optical bistability can therefore be observed within a window of detunings in the vicinity of the SQD transition frequency. The width of the window is typically on the order of several units/few dozens of Γ. In small SQDs the dipole dephasing time is usually strongly temperature dependent and can change from ns for low temperatures to less than ps for room temperature.[30] The bistability exists only if the feedback parameter G exceeds some threshold value. If $G_\mathrm{I} = 0$ the condition for bistability to occur is $G_\mathrm{R} \geq 4\Gamma$[26] while if $G_\mathrm{R} = 0$ the condition is $G_\mathrm{I} \geq 8\Gamma$.[31] The value of G is determined by the geometry and material properties and can not be increased arbitrarily. Therefore, these criteria can be used to choose suitable materials and system configuration.

We note that only the population difference Z manifests the standard S-shape curves while all the quantities related to the SQD dipole amplitude R exhibit more exotic coiled curves. As we show below, the latter leads to completely different types of hysteresis loops for these quantities.

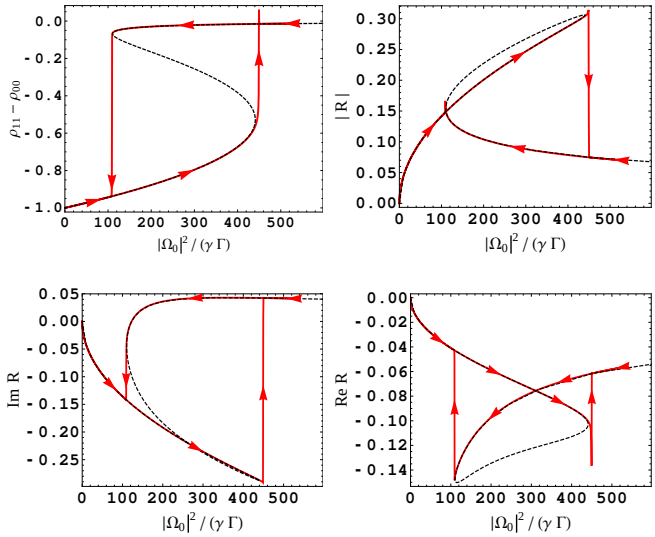

FIG. 4: Optical hysteresis loops of the population difference $Z = \rho_{11} - \rho_{00}$ and the SQD dipole moment amplitude R obtained by solving Eqs. (1a) and (1b) with the external field intensity $|\Omega_0|^2/\sqrt{\gamma\Gamma}$ being adiabatically swept back and forth across the bistability region (the sweeping speed of the renormalized Rabi frequency $\widetilde{\Omega}_0/\sqrt{\gamma\Gamma}$ is $2.1\times10^{-3}\Gamma$) The detuning from the resonance is $\Delta = 1.5\Gamma$. All other parameters are as in Fig. 3.

IV. OPTICAL HYSTERESIS

We performed time-domain calculations with the external field intensity $|\Omega_0|^2/(\gamma\Gamma)$ being adiabatically swept back and forth across the bistability region (the sweeping speeds are given in figure captions), monitoring the evolution of the system to figure out which steady state branches are stable. The results are shown in Fig. 4. For the population difference Z and the absorptive part of the SQD dipole moment $\mathrm{Im}(R)$ we find the standard behavior. Upon increasing the applied intensity, the system follows the lower (stable) branch until the intensity reaches the critical value at which the system switches to the upper branch (which is also stable). Upon sweeping the intensity back, the system stays on the upper branch and then switches back down to the lower one at the other critical intensity, completing the hysteresis loop. The intermediate branch can not be revealed by the adiabatic sweeping of the field because it is unstable which can also be checked by the standard stability analysis.

Both the $|R|$ and the $\mathrm{Im}(R)$ behave in a very different manner, manifesting hysteresis loops with kinks. In the case of the $|R|$ the upper branch is unstable and the hysteresis loop is triangular, while the $\mathrm{Im}(R)$ with its unstable lower branch has even more complicated bow-tie hysteresis curve. To the best of our knowledge no such optical hysteresis loops have neither been predicted nor observed so far.

These unusual properties are also expected to manifest themselves in the MNP dipole moment because it depends on that of the SQD [see Eq. (3)] and can therefore be switched abruptly as well.

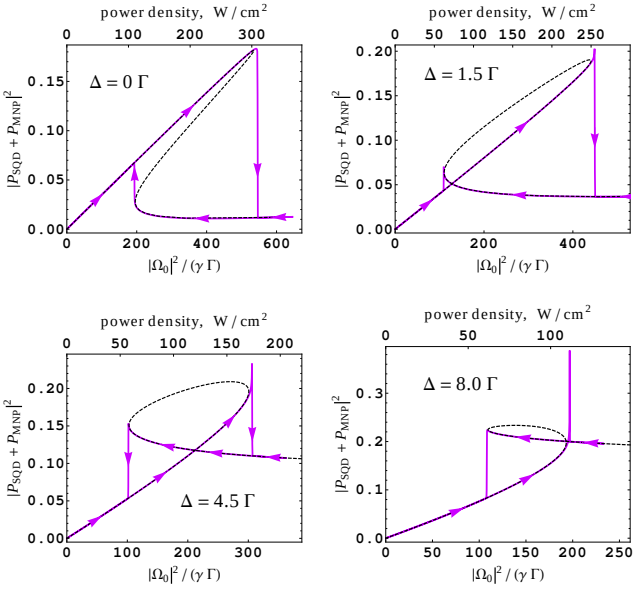

FIG. 5: The Rayleigh scattering intensity $|P_{\mathrm{SQD}} + P_{\mathrm{MNP}}|^2$ in units of $|\mu|^2$ for different values of Δ (indicated in the figures) as a function of excitation intensity. The corresponding power density is shown in the upper axis. Sweeping speeds of the renormalized Rabi frequency $\widetilde{\Omega}_0/\sqrt{\gamma\Gamma}$ in units of Γ is on the order of 10^{-3} for all values of Δ. All other parameters are as in Fig. 3.

V. RAYLEIGH SCATTERING AND OPTICAL STORAGE

In experiment, the intensity of the Rayleigh scattering can be measured. The amplitude of this characteristic is known to be proportional to the squared absolute value of the total system dipole moment $|P_{\mathrm{SQD}} + P_{\mathrm{MNP}}|^2$ and is therefore expected to manifest bistability as well. We plot the amplitude of the Rayleigh scattering in Fig. 5 for different values of the detuning Δ. The figure shows that various types of hysteresis curves can be observed: the standard loop (for $\Delta = 0$) as well as more exotic triangular loops ($\Delta = 1.5\,\Gamma$ and $\Delta = 8\,\Gamma$) and the bow-tie one ($\Delta = 4.5\,\Gamma$). The two latter types of hysteresis curves are characteristic for the SQD dipole moment (see Fig. 4), which suggests that the major contribution to the scattering is coming from the SQD. To confirm the latter we calculated the relative contribution of the SQD dipole moment into the total scattering amplitude, $|P_{\mathrm{SQD}}|^2/|P_{\mathrm{SQD}} + P_{\mathrm{MNP}}|^2$ which turned up to be on the order of unity across the whole hysteresis region. Within this region the contribution of the MNP to the scattered field is typically an order of magnitude less than that of the SQD for the chosen set of parameters.

It is to be noticed that the ratio of the scattering intensity in the two stable states can be as high as about 25 for $\Delta = 0$. Such high contrast suggests that the system can be used as an optical memory cell: lower intensity can represent a logical zero while the higher – a logical one. The state of the cell can be switched by sweeping the excitation power across the bistability region. Another possibility to switch the cell is to maintain the power constant while changing the incident field polarization. The latter mechanism is characteristic for this particular system due to its axial symmetry. We point out that such memory is a volatile one as it requires constant pumping.

VI. SUMMARY

We investigated theoretically the optical response of a hybrid "artificial molecule" comprised of a closely spaced spherical semiconductor quantum dot (modeled as a two-level system) and a metal nanosphere (considered classically), which are coupled by the dipole-dipole interaction. The interaction results in self-action of the SQD via the MNP, leading to the population dependence of the SQD transition frequency and relaxation constant of the SQD dipole moment. This provides a feedback mechanism resulting in several fascinating effects. Thus, we found that the system can manifest bistability and optical hysteresis. In particular, the total dipole moment of the system can be switched between its two stable states by the incoming field. The latter suggests such possible applications as optical memory cells and all-optical switches at nanoscale in the visible.

Because the SQD-MNP dipole-dipole interaction depends orientation of the dipole moments of the two particles, the switching can be achieved not only by the traditional control by the incident amplitude, but also by changing the polarization of the incoming field with respect to the system axis. Our calculations performed for typical system parameters, such as those of a CdSe or CdSe/ZnSe quantum dot and an Au nanoparticle complexes, predict the optical bistability of a SQD-MNP artificial molecule. The Rayleigh scattering and modern methods of single molecule/particle spectroscopy[30,32–34] could probably be used to discover the predicted effects experimentally.

To conclude, we considered the simplest diatomic hybrid artificial nano-molecule. We expect, however, that more complicated clusters (such as an SQD surrounded by several MNPs, as considered in Ref. 15) can also ex-

hibit these effects because in such systems nanoparticles are just playing the role of a "resonator" and provide feedback to the nonlinear two-level system. Anisotropy of nanoparticles can also easily be accounted for by using an appropriate tensor instead of the scalar polarizability. Finally, we note that a very interesting aspect of this kind of systems is the direction of the total induced dipole moment, which can also be bistable.

VII. ACKNOWLEDGMENTS

A. V. M. acknowledges support from projects MOSAICO (FIS2006-01485), BSCH-UCM (PR58/08), the Ramón y Cajal program (Ministerio de Ciencia e Innovación de España) and is grateful to the University of Groningen for hospitality.

* Electronic address: a.malyshev@fis.ucm.es

[1] M. Quinten, A. Leitner, R.M. Krenn, and F.R. Aussenegg, Opt. Lett. **23**, 1331 (1998).
[2] M. L. Brongersma, J. W. Hartman, and H. A. Atwater, Phys. Rev. B **62**, R16356 (2000).
[3] K. Li, M. I. Stockman, and D. J. Bergman, Phys. Rev. Lett. **91**, 227402 (2003).
[4] M. I. Stockman, Phys. Rev. Lett. **93**, 137404 (2004).
[5] D. S. Citrin, Nano Lett. **4**, 1561 (2004).
[6] J. V. Hernández, L. D. Noordan, and F. J. Robicheaux, J. Phys. Chem. B **109**, 15808 (2005).
[7] R. René de Waele, A. F. Koenderink, and A. Polman, Nano Lett. **7**, 2004 (2007).
[8] A. V. Malyshev, V. A. Malyshev, and J. Knoester, Nano Lett. **8**, 2369 (2008).
[9] M. J. Zheng, J. J. Xiao, and K. W. Yu, J. Appl. Phys. **106**, 113307 (2009).
[10] S. A. Maier, *Plasmonics: Fundamentals and Applications*, Springer: New York, 2007.
[11] T. Pons, I. L. Medintz, K. E. Sapsford, S. Higashiya, A. F. Grimes, D. S. English, and H. Mattoussi, Nano Lett. **7**, 3157 (2007).
[12] W. Zhang, A. O. Govorov, and G.W. Bryant, Phys. Rev. Lett. **97**, 146804 (2006).
[13] R. D. Artuso and G. V. Bryant, Nano Lett. **8**, 2106 (2008).
[14] R. D. Artuso and G. W. Bryant, Phys. rev B **82**, 195419 (2010).
[15] A. O. Govorov, G. W. Bryant, W. Zhang, T. Skeini, J. Lee, N. A. Kotov, J. M. Slocik, and R. R. Naik, Nano Lett. **6**, 984 (2006).
[16] S. M. Sadeghi, Phys. Rev. B **79**, 233309 (2009).
[17] S. M. Sadeghi, Nanotechnology **20**, 225401 (2009).
[18] S. M. Sadeghi, Nanotechnology **21**, 355501 (2010).
[19] S. M. Sadeghi, Nanotechnology **21**, 455401 (2010).
[20] J.-Y. Yan, W. Zhang, S. Duan, X.-G. Zhao, A. O. Govorov, Phys. Rev. B **77**, 165301 (2008).
[21] V. A. Malyshev, H. Glaeske, and K.-H. Feller, Phys. Rev. A **58**, 1496 (1998).
[22] Batygin V. V., Toptygin I. N. *Sbornik Zadach Po Elektrodinamike 2-e izd.* (M.: Nauka, 1970); *Problems In Electrodynamics* 2nd ed.; Academic Press, London, 1978.
[23] C. F. Bohren and D. R. Huffman, *Absorption and Scattering of Light by Small Particles*, Wiley: New York, 1983.
[24] M. Meier and A. Wokaun, Opt. Lett. **8**, 581583 (1983).
[25] A. I. Ekimov *et*. al., J. Opt. Soc. Am. B **10**, 100 (1993). k
[26] R. Friedberg, S. R. Hartmann, and J. T. Manassah, Phys. Rev. A **39**, 3444 (1989).
[27] M. G. Benedict, V. A. Malyshev, E. D. Trifonov, and A. I. Zaitsev, Phys. Rev. A **43**, 3845 (1991).
[28] V. Malyshev and P. Moreno, Phys. Rev. A **53**, 416 (1996).
[29] P. B. Johnson and R. W. Christy, Phys. Rev. B **6**, 4370 (1972).
[30] X. Michalet, F. Pinaud, T. D. Lacoste, M. Dahan, M. P. Bruchez, A. P. Alivisatos, and S. Weiss, Single Mol. **2**, 261 (2001).
[31] A. M. Basharov, Zh. Exp. Teor. Fiz. **94**, 12 (1988) [Engl. transl.: Sov. Phys. JETP **67**, 1741 (1988).
[32] L. J. E. Anderson, K. M. Mayer, R. D. Fraleigh, Y. Yang, S. Lee, and J. H. Hafner, J. Phys. Chem. C **114**, 11127 (2010).
[33] A. Tcherniak, J. W. Ha, S. Dominguez-Medina, L. S. Slaughter, and S. Link S, Nano Lett. **10**, 1398 (2010).
[34] L. S. Slaughter, W.-S. Chang, P. Swanglap, A. Tcherniak, B. P. Khanal, E. R. Zubarev, and S. Link, J. Phys. Chem. C **114**, 4934 (2010).